Cooling and squeezing the fluctuations of a nanomechanical beam by indirect quantum feedback control

Jing Zhang,[1,2,*] Yu-xi Liu,[1,3,4] and Franco Nori[1,3,5]

[1]*Advanced Science Institute, The Institute of Physical and Chemical Research (RIKEN), Wako-shi, Saitama 351-0198, Japan*
[2]*Department of Automation, Tsinghua University, Beijing 100084, People's Republic of China*
[3]*CREST, Japan Science and Technology Agency (JST), Kawaguchi, Saitama 332-0012, Japan*
[4]*Institute of Microelectronics, Tsinghua University, Beijing 100084, People's Republic of China*
[5]*Center for Theoretical Physics, Physics Department, Center for the Study of Complex Systems, The University of Michigan, Ann Arbor, Michigan 48109-1040, USA*

(Received 19 February 2009; published 1 May 2009)

We study cooling and squeezing the fluctuations of a nanomechanical beam using quantum feedback control. In our model, the nanomechanical beam is coupled to a transmission line resonator via a superconducting quantum interference device. The leakage of the electromagnetic field from the transmission line resonator is measured using homodyne detection. This measured signal is then used to design a quantum feedback control signal to drive the electromagnetic field in the transmission line resonator. Although the control is imposed on the transmission line resonator, this quantum feedback control signal indirectly affects the thermal motion of the nanomechanical beam via the inductive beam-resonator coupling, making it possible to cool and squeeze the fluctuations of the beam, allowing it to approach the standard quantum limit.

DOI: 10.1103/PhysRevA.79.052102 PACS number(s): 03.65.Ta, 85.25.−j, 42.50.Lc

I. INTRODUCTION

Nanomechanical oscillators have recently attracted considerable attention for their possible applications in quantum information and quantum measurement (see, e.g., Refs. [1–33]). A nanomechanical oscillator is also a promising device for studying macroscopic quantum effects in mechanical systems (see, e.g., Refs. [1–10]). Using current experimental techniques (see, e.g., Refs. [3,11,12]), high-frequency nanomechanical oscillators ($\omega/2\pi\sim 1$ GHz) with quality factors Q in the range of 10^3–10^5 can be realized at low temperatures T on the order of millikelvin. When the vibrational energy $\hbar\omega$ of the nanomechanical oscillator becomes smaller than the thermal energy k_BT, the oscillator can be said to work in the quantum regime.

To observe quantum behavior in nanomechanical oscillators, e.g., quantum fluctuations or squeezing effects, the oscillator must be cooled to extremely low temperatures to approach the standard quantum limit. There have been numerous studies, both theoretical and experimental (see, e.g., Refs. [13–41]), investigating the cooling of the fluctuations of nanomechanical oscillators. Many of these studies focus on optomechanical systems (see, e.g., Refs. [13–23]), where an oscillating cantilever or an oscillating micromirror is modeled as a harmonic oscillator. There are two approaches in optomechanical cooling: passive cooling [13–20] and active cooling [21–23]. In passive cooling techniques, the mechanical oscillator is self-cooled by the dynamical back action, e.g., the radiation-pressure-induced back action [14–20] coming from the mirror surface of the optical cavity. In fact, for a high-finesse cavity, the photons reflected from the mirror of the cavity transfer momentum and induce additional damping to the mechanical oscillator. In active cooling techniques, the reflected signal coming from the mechanical oscillator is sent to an electronic circuit, e.g., a derivative circuit, to provide a modulating signal, which is then used to control the back-action force imposed on the mechanical oscillator. Since the cooling effect can be actively controlled by tuning the feedback gain obtained in the control circuit, this is called an active cooling strategy.

Although it has recently been reported that ground-state cooling [24–27] could be realized in optomechanical systems, it is difficult to observe the macroscopic quantum effects of the mechanical oscillators in these optomechanical systems using current experimental conditions. The main difficulty comes from the fact that the characteristic oscillating frequency of the mechanical oscillator in these systems is not high enough (typically on the order of kilohertz or megahertz), and the corresponding effective temperature to observe the quantum effects is extremely low (typically on the order of nanokelvin or microkelvin), which is difficult to realize in present-day experiments.

Besides optomechanical cooling, a nanomechanical oscillator can also be embedded in an electronic circuit and cooled by coupling it to an electronic system [28–30]. Possible strategies include nanomechanical oscillators coupled to superconducting single-electron transistors [31,32], quantum dots [33,34], Josephson-junction superconducting circuits [35–39], or transmission line resonators [40,41]. Compared with mechanical oscillators in optical systems, a high-frequency oscillator can be realized more easily in electronic systems. Indeed, it has been reported that nanomechanical beams [11,12] with frequencies in the regime of gigahertz have been realized, and these beams seem to be suitable for integration in an electronic circuit. Since the effective temperature of such a mechanical oscillator can be in the millikelvin regime, it should be possible to observe quantum behavior in this case.

Like optomechanical systems, active feedback controls can be introduced to cool the motions of the nanomechanical

*jing-zhang@mail.tsinghua.edu.cn

oscillators in electronic systems. In the theoretical proposal in Ref. [32], a nanomechanical resonator is capacitively coupled to a single-electron transistor to measure the position of the resonator. The information obtained by the quantum measurement is fed into a feedback circuit to obtain an output control signal, which is then imposed on a feedback electrode to control the motion of the resonator. In this strategy, the quantum measurement and the designed feedback control introduce additional damping effects on the resonator, which are helpful for cooling the motion of the resonator.

In a recent experiment [42], a nanomechanical beam acted as one side of a superconducting quantum interference device (SQUID), and the voltage across the SQUID was measured which can be used to detect the motion of the beam. Motivated by this experiment, here we study the coupling between such a system [42] and a transmission line resonator. A single-mode quantized electromagnetic field provided by this resonator [43] could be detected by a homodyne measurement [44]. The quantization of this coupled beam-SQUID-resonator system has been addressed in the literature (see, e.g., Refs. [45–47]), and theoretical analysis shows that such a device can be used to detect the motion of the beam [47]. Here, we would like to concentrate on a different problem: how to design a quantum feedback control from the output signal of the homodyne detection to drive the motion of the beam? Different from previous work, such as the one in Ref. [32], the quantum feedback control proposed here is *imposed on the transmission line resonator, not on the beam*, and indirectly controls the motion of the nanomechanical beam via the coupling between the transmission line resonator and the beam. By adiabatically eliminating the degrees of freedom of the SQUID and the transmission line resonator, the designed feedback control could introduce anharmonic terms in the effective Hamiltonian and additional damping terms for the nanomechanical beam, *leading to both cooling and squeezing* of the fluctuations of the beam.

Our studies indicate that the nanomechanical beam can be cooled from about 100 mK (the approximate temperature of the environment) to about 5 mK. However, the cooling achieved might not be sufficient for the beam to reach its ground-state energy. Also, note that in our proposal the energy flows from the beam to the transmission line resonator via the SQUID, and then, from the transmission line resonator, flows out into the vacuum. This energy flow is because k_BT is larger than the energy gap of the beam (so the beam is thermally excited), but k_BT is smaller than the energy gap of the transmission line resonator (so the resonator is not thermally excited).

Generally, squeezing a quantum state [48] requires injecting energy into a system in order to suppress fluctuations. Our proposed device injects energy, modulated by feedback control, into the transmission line resonator, in order to squeeze the fluctuations of the beam. Indeed, without control, the equilibrium state of the beam is a thermal state, and the energy injected into the system would drive the beam away from this equilibrium state. Suppressing the fluctuations of the beam displacement first cools the system and then, for sufficiently low temperatures, squeezes its state.

This paper is organized as follows: in Sec. II, we present a coupled system composed of (i) a transmission line resonator, (ii) an rf SQUID, and (iii) a nanomechanical beam. The open quantum system model and the quantum weak measurement approach used to design the feedback control are investigated in Sec. III. The quantum feedback control design is presented in Sec. IV, and our main results about squeezing and cooling the fluctuations of the beam are discussed in Sec. V. The conclusion and discussion of possible future work are presented in Sec. VI.

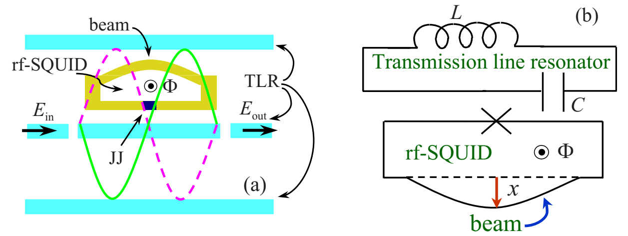

FIG. 1. (Color online) (a) Schematic diagram of a transmission line resonator (TLR), in blue, and a SQUID-nanomechanical beam system, in dark yellow and dark blue. Here, "JJ" represents a Josephson junction and E_{in}, E_{out} are, respectively, the input and output electromagnetic fields of the transmission line resonator. (b) Diagram of the quantum circuit.

II. SYSTEM MODEL AND HAMILTONIAN

We mainly focus on a physical model in which a doubly-clamped nanomechanical beam, a rf SQUID, and a transmission line resonator are inductively coupled (see, e.g., Refs. [45–47]). The quantum electromechanical circuit and the corresponding equivalent schematic diagram are shown in Fig. 1. In this circuit, the mechanical oscillator, i.e., the clamped nanomechanical beam, is integrated into the rf SQUID with a Josephson junction having a critical current I_c and a capacitance C. Here, the displacement of the beam in the plane of the loop with a small amplitude x around its equilibrium position changes the area of the loop and thus influences the total magnetic flux Φ threading the loop. There is an applied external flux Φ_e threading the loop. The rf SQUID interacts with a nearby transmission line resonator (TLR) via their mutual inductance. The additional magnetic flux provided by the quantized current in the transmission line resonator is

$$\Phi_{\text{add}} = \Phi_T(-ia + ia^\dagger),$$

where Φ_T is a constant and a and $a^\dagger$ are the annihilation and creation operators of the quantized electromagnetic field in the transmission line resonator. Here, we ignore the small change in Φ_T caused by the oscillation of the beam. For this superconducting circuit, the total magnetic flux Φ threading the loop of the rf SQUID is given by

$$\Phi = \Phi_e + Blx + \Phi_T(-ia + ia^\dagger) + LI,$$

where L and I are, respectively, the self-inductance and the current in the loop, l is the effective length of the beam, and B is the magnetic field threading the loop of the rf SQUID at the location of the nanomechanical beam and is assumed to be constant in the region where the beam oscillates.

The total Hamiltonian of this coupled electromechanical system can be written as [46]

$$H = H_0 + H_1, \tag{1}$$

with the Hamiltonians

$$H_0 = \frac{p^2}{2m} + \frac{m\omega_M^2 x^2}{2} + \hbar\omega_T a^\dagger a + \hbar u(t)(a^\dagger + a), \tag{2}$$

$$H_1 = U_0\left[\phi - \phi_e - \kappa(-ia + ia^\dagger) - \frac{2\pi Bl}{\Phi_0}x\right]^2 + 2U_0\beta_L \cos\phi + \frac{q^2}{2C}, \tag{3}$$

where Φ_0 is the flux quantum, ω_T is the frequency of the electromagnetic field in the transmission line resonator, ω_M is the oscillating frequency of the doubly-clamped beam, and ϕ and ϕ_e are related to the normalized total flux and external flux,

$$\phi = 2\pi\left(\frac{\Phi}{\Phi_0} - \frac{1}{2}\right), \quad \phi_e = 2\pi\left(\frac{\Phi_e}{\Phi_0} - \frac{1}{2}\right). \tag{4}$$

The normalized system parameters U_0, β_L, and κ in Eq. (1) are given by

$$U_0 = \frac{\Phi_0^2}{8\pi L}, \quad \beta_L = \frac{2\pi L I_c}{\Phi_0}, \quad \kappa = \frac{2\pi\Phi_T}{\Phi_0}.$$

The observables p and q in Eqs. (2) and (3) are, respectively, the conjugate observables of x and Φ representing the momentum of the beam and the charge on the Josephson junction. The term $\hbar u(t)(a^\dagger + a)$ in Eq. (2) is an interaction Hamiltonian between the transmission line resonator and the external control field, where the time-dependent function $u(t)$ can be designed according to the desired goal.

When $\beta_L > 1$ and

$$\left|\phi_e + \frac{2\pi Blx}{\Phi_0} + \kappa(-ia + ia^\dagger)\right| = |\phi_e'| \ll 1, \tag{5}$$

the Hamiltonian H_1 represents a double-well potential near $\phi=0$, and the two lowest eigenstates, $|L\rangle$ and $|R\rangle$, correspond to two current states with opposite circulating currents in the loop of the rf SQUID, which are far separated from higher-energy eigenstates. At sufficiently low temperatures, only the two lowest eigenstates $|L\rangle$, $|R\rangle$ contribute. Thus, the rf SQUID can be modeled as a two-level system, and the Hamiltonian H_1 of the rf SQUID can be re-expressed as [46]

$$H_1 = \frac{\hbar\epsilon}{2}\left(\phi_e + \frac{2\pi Bl}{\Phi_0}x + \kappa(-ia + ia^\dagger)\right)\tilde{\sigma}_z - \frac{\hbar\Delta}{2}\tilde{\sigma}_x,$$

where $\tilde{\sigma}_x$ and $\tilde{\sigma}_z$ are the x-axis and z-axis Pauli operators in the basis of $|L\rangle$ and $|R\rangle$ and ϵ and Δ are real parameters that determine the energy difference between the two minima of the double-well potential and the tunneling amplitude between the wells, respectively. Under the condition that

$$0 < (\beta_L - 1) \ll 1,$$

then ϵ and Δ can be approximately given by [49]

$$\epsilon = \frac{I_c\Phi_0}{\hbar\pi}\sqrt{6(\beta_L - 1)}, \quad \Delta = 3U_0\left(1 - \frac{1}{\beta_L}\right)^2. \tag{6}$$

Let the normalized external flux $\phi_e=0$, i.e., in Eq. (4) the applied external magnetic field $\Phi_e=\Phi_0/2$. This means that the qubit (the rf SQUID) is at the degeneracy point when there is no coupling between the qubit and the nanomechanical beam as well as no coupling between the qubit and the transmission line resonator. Then, we can rewrite the Hamiltonian H_1 in the qubit basis as

$$H_1 = \frac{\hbar\omega_S}{2}\sigma_z + \frac{\hbar\pi\epsilon Bl}{\Phi_0}x\sigma_x + \frac{\hbar\kappa\epsilon}{2}(-ia + ia^\dagger)\sigma_x, \tag{7}$$

where $\omega_S=\Delta$ and σ_x and σ_z are the corresponding x-axis and z-axis Pauli operators in the qubit basis,

$$|+\rangle = \frac{\sqrt{2}}{2}|L\rangle + \frac{\sqrt{2}}{2}|R\rangle,$$

$$|-\rangle = \frac{\sqrt{2}}{2}|L\rangle - \frac{\sqrt{2}}{2}|R\rangle.$$

Here, we assume that the oscillation frequency of the beam is high enough such that ω_M, ω_S, and ω_T are comparable. Then, under the rotating-wave approximation and with Eq. (7), the total Hamiltonian in Eq. (1) becomes

$$H = \frac{\hbar\omega_S}{2}\sigma_z + \hbar\omega_M b^\dagger b + \hbar\omega_T a^\dagger a + \hbar u(t)(a^\dagger + a) + \hbar g_{MS}(b\sigma_+ + \sigma_- b^\dagger) + \hbar g_{ST}(-ia\sigma_+ + i\sigma_- a^\dagger), \tag{8}$$

where the coupling strength g_{MS} between the mechanical oscillator and the rf SQUID is

$$g_{MS} = g_{\text{mech-SQUID}} = \frac{\pi\epsilon Bl}{\Phi_0\sqrt{2\hbar m\omega_M}},$$

and the coupling strength g_{ST} between the rf SQUID and the transmission line resonator is given by

$$g_{ST} = g_{\text{SQUID-TLR}} = \frac{\kappa\epsilon}{2\hbar}.$$

The annihilation and creation operators b and $b^\dagger$ of the fundamental oscillating mode of the nanomechanical beam are defined by

$$b = \sqrt{\frac{m\omega_M}{2\hbar}}x + i\frac{1}{\sqrt{2\hbar m\omega_M}}p,$$

$$b^\dagger = \sqrt{\frac{m\omega_M}{2\hbar}}x - i\frac{1}{\sqrt{2\hbar m\omega_M}}p.$$

Furthermore, let us assume that the frequencies of the rf SQUID, the beam, and the transmission line resonator satisfy the conditions

$$g_{MS} \ll \Delta_{MS} = \omega_S - \omega_M, \quad g_{ST} \ll \Delta_{ST} = \omega_S - \omega_T. \tag{9}$$

Then, in this large-detuning regime [50], the following transformation can be introduced to diagonalize the Hamiltonian H in Eq. (8):

$$U = \exp\left[\frac{g_{MS}}{\Delta_{MS}}(b\sigma_+ - b^\dagger\sigma_-) - \frac{g_{ST}}{\Delta_{ST}}(ia\sigma_+ + ia^\dagger\sigma_-)\right].$$

In fact, under the condition given in Eq. (9), we can obtain an effective Hamiltonian,

$$\begin{aligned} H_{\mathrm{eff}} &= UHU^\dagger \\ &\approx \hbar\omega_M b^\dagger b + \hbar\omega_T a^\dagger a + \hbar u(t)(a^\dagger + a) \\ &\quad + \frac{\hbar\omega_S}{2}\sigma_z + \hbar\left(\frac{g_{MS}^2}{\Delta_{MS}}b^\dagger b + \frac{g_{ST}^2}{\Delta_{ST}}a^\dagger a\right)\sigma_z \\ &\quad + \hbar\left(\frac{g_{MS}g_{ST}}{\Delta_{MS}} + \frac{g_{MS}g_{ST}}{\Delta_{ST}}\right)(-iba^\dagger + ib^\dagger a)\sigma_z \end{aligned}$$

by expanding $UHU^\dagger$ to first order in g_{MS}/Δ_{MS} and g_{ST}/Δ_{ST}.

III. INTERACTION BETWEEN THE SYSTEM AND ITS ENVIRONMENT

Any physical system inevitably interacts with the external degrees of freedom in the environment. Such interactions introduce noise to the system. There are three kinds of noise that will be considered here: the thermal noises on the nanomechanical beam and the transmission line resonator, as well as the electromagnetic fluctuations on the rf SQUID caused by the nearby electromagnetic elements.

Let us consider a bosonic model of the environment and assume that the interaction between the system and the environment is linear. Then, under the rotating-wave approximation, the Hamiltonian of the total system, composed of the coupled beam-SQUID-resonator system and the environment, can be expressed as

$$\begin{aligned} H_{\mathrm{tot}} &= H_{\mathrm{eff}} + \int \hbar\omega c_{pT}^\dagger c_{pT} d\omega + \int \hbar\omega c_{eT}^\dagger c_{eT} d\omega \\ &\quad + \int \hbar\omega c_{eM}^\dagger c_{eM} d\omega + \int \hbar\omega c_{eS}^\dagger c_{eS} d\omega \\ &\quad + \hbar\int d\omega[g_{pT}^*(\omega)c_{pT}^\dagger a + g_{pT}(\omega)a^\dagger c_{pT}] \\ &\quad + \hbar\int d\omega[g_{eT}^*(\omega)c_{eT}^\dagger a + g_{eT}(\omega)a^\dagger c_{eT}] \\ &\quad + \hbar\int d\omega[g_{eM}^*(\omega)c_{eM}^\dagger b + g_{eM}(\omega)b^\dagger c_{eM}] \\ &\quad + \hbar\int d\omega[g_{eS,\varphi}^*(\omega)c_{eS,\varphi}^\dagger \sigma_z + g_{eS}(\omega)\sigma_z c_{eS}] \\ &\quad + \hbar\int d\omega[g_{eS}^*(\omega)c_{eS,r}^\dagger \sigma_- + g_{eS,r}(\omega)\sigma_+ c_{eS}], \end{aligned}$$

where the terms in the first and second lines of the above equation are the free Hamiltonians of the system and the environment with c_{pT} ($c_{pT}^\dagger$), c_{eT} ($c_{eT}^\dagger$), c_{eM} ($c_{eM}^\dagger$), and c_{eS} ($c_{eS}^\dagger$) denoting the annihilation (creation) operators of different environmental degrees of freedom, which satisfy

$$[c_i(\omega), c_j^\dagger(\omega')] = \delta_{ij}\delta(\omega - \omega').$$

The other terms in H_{tot} represent the interactions between the transmission line resonator, the nanomechanical beam, and the rf SQUID and their environments; g_{pT} and g_{eT} denote the strengths of the couplings between the transmission line resonator and the environmental degrees of freedom interacting when it is "probed" (pT) and not probed (eT); g_{eM} is the strength of the coupling between the mechanical beam and the environment; and $g_{eS,\varphi}$ and $g_{eS,r}$ represent the strengths of the couplings between the rf SQUID and the environment which lead to pure-dephasing and relaxation effects of the rf SQUID, respectively.

To clarify further the notation, we note that the subscripts pT and eT represent the environmental degrees of freedom interacting with the transmission line resonator being probed (pT) and not being probed (eT). The subscripts eM and eS denote the environmental (thus the e) degrees of freedom interacting with the mechanical beam and the SQUID, respectively.

Furthermore, under the Markovian approximation, we can obtain the following quantum stochastic differential equation for a system observable X (see Appendix A for the derivation):

$$\begin{aligned} dX &= -\frac{i}{\hbar}[X, H_{\mathrm{eff}}]dt + \frac{\gamma_{S\varphi}}{2}[\sigma_z, [X, \sigma_z]]dt \\ &\quad + \frac{\gamma_{Sr}}{2}(\sigma_+[X, \sigma_-] + [\sigma_+, X]\sigma_-)dt \\ &\quad + \frac{\gamma_M}{2}(\bar{n}_M + 1)(b^\dagger[X, b] + [b^\dagger, X]b)dt \\ &\quad + \frac{\gamma_M}{2}\bar{n}_M(b[X, b^\dagger] + [b, X]b^\dagger)dt \\ &\quad + \frac{\gamma_T}{2}(a^\dagger[X, a] + [a^\dagger, X]a)dt \\ &\quad + \sqrt{\eta\gamma_T}dA_{\mathrm{in}}^\dagger[X, a] + \sqrt{\eta\gamma_T}[a^\dagger, X]dA_{\mathrm{in}} \\ &\triangleq \mathcal{L}_{\mathrm{sys}}^*(X)dt + \sqrt{\eta\gamma_T}dA_{\mathrm{in}}^\dagger[X, a] + \sqrt{\eta\gamma_T}[a^\dagger, X]dA_{\mathrm{in}}, \end{aligned} \tag{10}$$

where $\mathcal{L}_{\mathrm{sys}}^*(\cdot)$ is the Liouville superoperator of the system in the Heisenberg picture, γ_M and γ_T are the damping rates of the mechanical beam and the transmission line resonator, $\gamma_{S\varphi}$ and γ_{Sr} are the pure-dephasing and relaxation rates of the rf SQUID under the Markovian approximation, and

$$\bar{n}_M = \frac{1}{e^{\hbar\omega_M/k_B T} - 1} \tag{11}$$

is the average photon number of the beam in thermal equilibrium with the environment at temperature T. To simplify our discussions, when Eq. (10) was derived, we neglected environment-induced thermal excitations on the transmission line resonator and the rf SQUID [these excitations could indeed be neglected with the parameters given in Eqs. (29) and (30) in Sec. V]. The leakage of the transmission line resonator could be detected using a homodyne detection with detection efficiency η, where dA_{in} represents a quantum Wiener noise [51] satisfying

$$dA_{\mathrm{in}}^{\dagger}dA_{\mathrm{in}} = dA_{\mathrm{in}}dA_{\mathrm{in}} = dA_{\mathrm{in}}^{\dagger}dA_{\mathrm{in}}^{\dagger} = 0,$$
$$dA_{\mathrm{in}}dA_{\mathrm{in}}^{\dagger} = dt.$$

Here, we only keep the fluctuation terms caused by the measurement and average over the other fluctuations because the evolution of the coupled beam-SQUID-resonator system is conditioned on the measurement output, which depends on the measurement-induced fluctuations. The corresponding measurement output of the homodyne detection can be expressed as [47]

$$dY_t = \sqrt{\eta\gamma_T}(a^{\dagger} + a) + (dA_{\mathrm{in}} + dA_{\mathrm{in}}^{\dagger}). \tag{12}$$

Note that this measurement output depends on the input noise and the electromagnetic field of the transmission line resonator.

IV. QUANTUM FILTERING AND QUANTUM FEEDBACK CONTROL

There are two possible ways to design a quantum feedback control protocol [52,53] based on the measurement output. One approach is to directly feed back the output signal to design the quantum feedback control signal, which leads to the Markovian quantum feedback control [54]. Another approach, which is called quantum Bayesian feedback control [55], can be divided into two steps: the first step is to find a so-called quantum filtering equation [56–58] to give an estimate of the state of the system from the measurement output; the second step is to design a feedback control signal based on the estimated state. The possibility for a "control problem" to be divided into these two steps, i.e., a separate filtering step and a control step, is called the separation principle in control theory, which has recently been developed for quantum control systems [57]. Compared with the Markovian quantum feedback control, the quantum Bayesian feedback control can be applied to more general systems. In our proposal, we will design the control using Bayesian feedback control.

In order to design a Bayesian quantum feedback control, we should first give an estimate of an arbitrary observable X of the system which evolves according to Eq. (10) based on the information gained from the measurement output given in Eq. (12). The natural choice of such an estimate is the conditional expectation

$$\pi_t(X) = E(X|\mathcal{Y}_t) \tag{13}$$

under the von Neumann algebra [57],

$$\mathcal{Y}_t = vN\{Y_s|t_0 \le s \le t\}, \tag{14}$$

spanned by the measurement outputs. *Indeed*, $\pi_t(X)$ is the least mean square estimate of the system observable X given the observations up to time t. The main subject of the quantum filtering theory, which has been well developed in the literature [56,57], is to find a recursive equation for the conditional expectation $\pi_t(X)$ (the filtering equation). From the existing studies [56,57], such a filtering equation can be written as

$$d\pi_t(X) = [\pi_t(a^{\dagger}X + Xa) - \pi_t(a^{\dagger} + a)\pi_t(X)] \times [dY_t - \pi_t(a^{\dagger} + a)dt] + \pi_t(\mathcal{L}_{\mathrm{sys}}^{*}(X))dt, \tag{15}$$

where the Liouville superoperator $\mathcal{L}_{\mathrm{sys}}^{*}(\cdot)$ is defined in Eq. (10).

Furthermore, we can convert Eq. (15) from the Heisenberg picture to the Schrödinger picture. To show this, let us define an estimated system density operator $\tilde{\rho}$ such that $\mathrm{tr}(X\rho_0) = \mathrm{tr}(X_0\tilde{\rho})$, where ρ_0 is the initial density operator of the system and X_0 is the corresponding system observable in the Schrödinger picture. Then, from Eq. (15), the estimated density operator $\tilde{\rho}$ evolves according to the following stochastic master equation:

$$\begin{aligned} d\tilde{\rho} = &-\frac{i}{\hbar}[H_{\mathrm{eff}},\tilde{\rho}]dt + \gamma_M\bar{n}_M\mathcal{D}[b^{\dagger}]\tilde{\rho}dt + \gamma_M(\bar{n}_M + 1)\mathcal{D}[b]\tilde{\rho}dt \\ &+ \gamma_{S\varphi}\mathcal{D}[\sigma_z]\tilde{\rho}dt + \gamma_{Sr}\mathcal{D}[\sigma_-]\tilde{\rho}dt + \gamma_T\mathcal{D}[a]\tilde{\rho}dt \\ &+ \sqrt{\eta\gamma_T}\mathcal{H}[a]\tilde{\rho}[dY_t - \sqrt{\eta\gamma_T}\langle(a^{\dagger} + a)\rangle dt], \end{aligned} \tag{16}$$

where $\langle A\rangle = \mathrm{tr}(A\tilde{\rho})$ is the average of A under $\tilde{\rho}$ and the superoperators $\mathcal{D}[c]\tilde{\rho}$ and $\mathcal{H}[c]\tilde{\rho}$ are defined by

$$\mathcal{D}[c]\tilde{\rho} = c\tilde{\rho}c^{\dagger} - \tfrac{1}{2}c^{\dagger}c\tilde{\rho} - \tfrac{1}{2}\tilde{\rho}c^{\dagger}c,$$

$$\mathcal{H}[c]\tilde{\rho} = c\tilde{\rho} + \tilde{\rho}c^{\dagger} - \langle(c + c^{\dagger})\rangle\tilde{\rho}.$$

The increment

$$dW = dY_t - \sqrt{\eta\gamma_T}\langle(a^{\dagger} + a)\rangle dt \tag{17}$$

in Eq. (16) is the innovation updated by the quantum measurement, which has been proved to be a classical Wiener increment satisfying

$$E(dW) = 0, \quad (dW)^2 = dt$$

for homodyne detection (see, e.g., Ref. [57]).

From Eq. (13), we have

$$\tilde{\rho} = E(\rho|\mathcal{Y}_t), \tag{18}$$

i.e., $\tilde{\rho}$ is the conditional expectation of the density operator ρ of the coupled beam-SQUID-resonator system. Since the von Neumann algebra $\mathcal{Y}_t$ defined in Eq. (14) represents the information obtained by the quantum measurement up to time t, the conditional expectation $\tilde{\rho}$ defined in Eq. (18) is the best estimate of the system's state obtained from the measurement output.

Generally, the stochastic master equation, i.e., the filter equation, is difficult to solve. However, for the system we discuss here, the stochastic master equation [Eq. (16)] is equivalent to a set of closed equations under the semiclassical approximation [see Eqs. (B3) and (B4) in Appendix B]. This set of equations can be integrated by a data acquisition processor (DAP) (see, e.g., Ref. [52]), which is composed of a digital signal processor (DSP) and analog-to-digital and

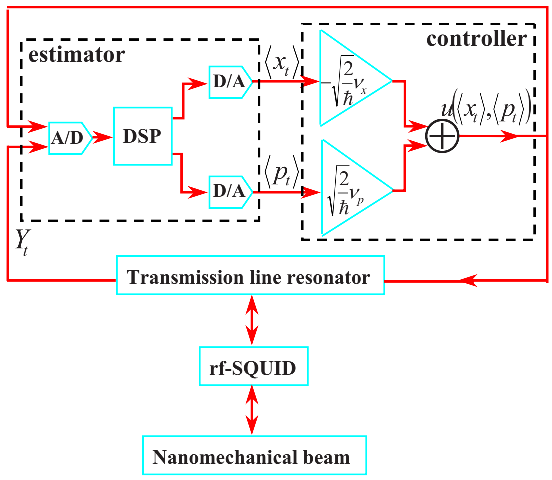

FIG. 2. (Color online) Schematic diagram of the feedback control circuit. The "DSP" denotes a digital signal processor which works as the integral estimator of the system state by solving Eqs. (B3) and (B4). The "A/D" and "D/A" represent the analog-to-digital and digital-to-analog signal converters. The output of the estimator is fed into a linear amplifier circuit to obtain a control signal which is further used to drive the input electromagnetic field of the transmission line resonator and the input of the estimator.

digital-to-analog signal converters. Such a data acquisition processor works as an integral estimator of the dynamics of the system state and gives the output signals $\langle x_T\rangle$ and $\langle p_T\rangle$. The output signals of the estimator are fed into a feedback controller (a linear amplification element) to obtain the following feedback control signal:

$$u(t)=\sqrt{\frac{2}{\hbar}}(-\upsilon_x\langle x_T\rangle+\upsilon_p\langle p_T\rangle), \tag{19}$$

where υ_x and υ_p are the feedback control gains that can be chosen according to the desired goal and x_T and p_T are the normalized position and momentum operators of the transmission line resonator defined by

$$x_T=\sqrt{\frac{\hbar}{2}}(a^\dagger+a),\quad p_T=\sqrt{\frac{\hbar}{2}}(-ia+ia^\dagger). \tag{20}$$

We replace $u(t)$ in Eqs. (10) and (16) by Eq. (19) to obtain new dynamical equations. In this case, we indeed control, simultaneously, the evolutions of the transmission line resonator and the estimator. The schematic diagram of the feedback control circuit is shown in Fig. 2. From definition (18) of $\tilde{\rho}$, it can be shown that the control of the coupled system given by Eq. (10) is equivalent to the control of the estimator given by Eq. (16). Thus, in the following discussion, we will focus on how to control the quantum filtering [Eq. (16)].

If the damping rates of the rf SQUID and the transmission line resonator are large enough such that

$$\tfrac{1}{2}\gamma_{Sr}+2\gamma_{S\varphi},\quad \gamma_T\gg\gamma_M\bar{n}_M, \tag{21}$$

we can adiabatically eliminate [59,60] the degrees of freedom of the rf SQUID and the transmission line resonator to obtain the following reduced stochastic master equation and the measurement output for the nanomechanical beam (see Appendix B for the derivation):

$$\begin{aligned}d\tilde{\rho}_M=&-\frac{i}{\hbar}[H_{\text{eff}}^{(M)},\tilde{\rho}_M]dt+\gamma_M\bar{n}_M\mathcal{D}[b^\dagger]\tilde{\rho}_M dt\\&+\gamma_M(\bar{n}_M+1)\mathcal{D}[b]\tilde{\rho}_M dt+\gamma_T\mathcal{D}[C_1b+C_2b^\dagger]\tilde{\rho}_M dt\\&+\sqrt{\eta\gamma_T}\mathcal{H}[C_1b+C_2b^\dagger]\tilde{\rho}_M dW,\end{aligned}$$

$$dY_t=\sqrt{\eta\gamma_T}\langle(\alpha_xb+\alpha_x^*b^\dagger)\rangle dt+dW, \tag{22}$$

where the reduced Hamiltonian $H_{\text{eff}}^{(M)}$ is given by

$$H_{\text{eff}}^{(M)}=\hbar\omega_Mb^\dagger b+\hbar\xi_Mb^2+\hbar\xi_M^*b^{\dagger 2}+\hbar\tilde{u}(t)(\alpha_xb+\alpha_x^*b^\dagger), \tag{23}$$

and the reduced effective control on the beam is

$$\tilde{u}(t)=-\upsilon_x\langle(\alpha_xb+\alpha_x^*b^\dagger)\rangle+\upsilon_p\langle(\alpha_pb+\alpha_p^*b^\dagger)\rangle.$$

The parameters α_x, α_p, and ξ_M can be expressed as

$$\alpha_x=C_1+C_2^*,$$

$$\alpha_p=-iC_1+iC_2^*,$$

$$\xi_M=\omega_TC_2^*C_1-ig_{MT}C_2^*,$$

where g_{MT} is given by Eq. (B2) and C_1 and C_2 are given by

$$C_1(\upsilon_x,\upsilon_p)=\frac{g_{MT}}{\chi}\left[\left(\upsilon_p+\frac{\gamma_T}{2}\right)-i(-\upsilon_x+\omega_T)\right],$$

$$C_2(\upsilon_x,\upsilon_p)=\frac{g_{MT}}{\chi}(\upsilon_p-i\upsilon_x),$$

$$\chi(\upsilon_x,\upsilon_p)=\frac{\gamma_T}{4}(\gamma_T+4\upsilon_p)+\omega_T(\omega_T-2\upsilon_x). \tag{24}$$

As shown in Eq. (23), there is a two-photon term $\hbar\xi_Mb^2+\hbar\xi_M^*b^{\dagger 2}$ in the effective Hamiltonian $H_{\text{eff}}^{(M)}$, which leads to squeezing in the fluctuations of the beam. Without the quantum feedback control, i.e., $\upsilon_x=\upsilon_p=0$, ξ_M would be zero and the two-photon term vanishes.

Equation (22) shows that the quantum measurement and feedback control introduce extra damping and fluctuation terms for the beam [the third and fourth lines in Eq. (22)]. These damping terms are important for squeezing and cooling the fluctuations of the beam.

V. SQUEEZING AND COOLING THE FLUCTUATIONS OF THE NANOMECHANICAL BEAM

In order to study the squeezing and cooling effects on the nanomechanical beam induced by the quantum feedback control, let us first define the normalized position and momentum operators of the nanomechanical beam,

$$x_M = \sqrt{\frac{\hbar}{2}}(b + b^\dagger), \quad p_M = \sqrt{\frac{\hbar}{2}}(-ib + ib^\dagger).$$

Then, from the reduced stochastic master equation [Eq. (22)], we can study the evolutions and the corresponding stationary values of the variances

$$V_{x_M} = \langle x_M^2 \rangle - \langle x_M \rangle^2, \quad V_{p_M} = \langle p_M^2 \rangle - \langle p_M \rangle^2 \tag{25}$$

of x_M and p_M.

A. Squeezing

The nanomechanical beam can be described by the conjugate variables x_M and p_M and is in a squeezed state if the corresponding variances of these variables defined in Eq. (25) satisfy $V_{x_M} < \hbar/2$ or $V_{p_M} < \hbar/2$, i.e., the variance of one of the two conjugate variables is below the standard quantum limit (see, e.g., Refs. [61–63]). Owing to the uncertainty principle which requires that $V_{x_M} V_{p_M} \geq \hbar^2/4$, squeezing the fluctuations of one of the two conjugate variables would lead to the dispersion of the fluctuations of the other conjugate variable.

If we choose the feedback control gains v_x and v_p to satisfy the conditions

$$0 < \frac{\gamma_T}{\gamma_T + 4v_p} \ll 1,$$

$$0 < \frac{\omega_T - 2v_x}{\omega_T} \ll 1,$$

$$0 < \frac{\gamma_T g_{MT}^2 \omega_T^2}{\omega_M} \ll \chi^2, \tag{26}$$

then the stationary variances $V_{x_M}^c$ and $V_{p_M}^c$ can be estimated as

$$V_{x_M}^c \approx \frac{\hbar}{2}\sqrt{\frac{\xi}{\eta}}, \quad V_{p_M}^c \approx \frac{\hbar}{2}\frac{1}{\sqrt{\xi\eta}}, \tag{27}$$

where

$$\xi = \frac{\omega_M - 2 \operatorname{Re} \xi_M}{\omega_M + 2 \operatorname{Re} \xi_M}, \quad \operatorname{Re} \xi_M \approx \frac{\omega_T g_{MT}^2}{\chi^2}(v_p^2 - v_x^2). \tag{28}$$

It is shown in Eq. (27) that the parameter ξ determines the trade-off of the squeezing effects between V_{x_M} and V_{p_M}. When $\xi > 1$, the fluctuation of the momentum p_M of the nanomechanical beam is squeezed. However, when $\xi < 1$, the fluctuation of the position x_M of the nanomechanical beam is squeezed. The parameter η, i.e., the measurement efficiency of the homodyne detection, determines the minimum uncertainty that can be reached. For a quantum weak measurement with a high efficiency η such that

$$\frac{1}{(2\bar{n}_M + 1)^2} < \eta < 1,$$

where $\bar{n}_M$ is the thermal excitation number of the beam given in Eq. (11), it can be verified that

$$\frac{\hbar^2}{4} < V_{x_M}^c V_{p_M}^c \approx \frac{\hbar^2}{4\eta} < V_{x_M}^{uc} V_{p_M}^{uc} = \hbar^2 \left(\bar{n}_M + \frac{1}{2}\right)^2,$$

where $V_{x_M}^{uc}$ and $V_{p_M}^{uc}$ are the "uncontrolled" stationary variances that are obtained from Eq. (22) by letting $v_x = v_p = 0$. It should be pointed out that *the product of the uncertainties of* x_M and p_M given by Eq. (27), i.e.,

$$V_{x_M}^c V_{p_M}^c \approx \frac{\hbar^2}{4\eta},$$

corresponds to the *Heisenberg uncertainty limit of a quantum system* under imperfect quantum weak measurements (see, e.g., Ref. [64]). When the measurement efficiency η tends to unity, the traditional Heisenberg uncertainty limit $\hbar^2/4$ is recovered.

In order to obtain our main results, i.e., Eq. (27), we have assumed some restrictions on the system parameters and the feedback gains, which can be summarized as follows:

(i) The thermal excitation and the energy gaps of the mechanical beam, the rf SQUID, and the transmission line resonator satisfy the following condition:

$$\hbar\omega_T, \ \hbar\omega_S \gg k_B T > \hbar\omega_M.$$

(ii) We assumed a large detuning between the mechanical beam and the rf SQUID, as well as a large detuning between the transmission line resonator and the rf SQUID,

$$g_{MS} \ll \Delta_{MS} = \omega_S - \omega_M,$$

$$g_{ST} \ll \Delta_{ST} = \omega_S - \omega_T.$$

(iii) We considered the adiabatic elimination assumption: the damping rates of the rf SQUID and the transmission line resonator are far larger than the damping rate of the nanomechanical beam, i.e.,

$$\tfrac{1}{2}\gamma_{Sr} + 2\gamma_{S\varphi}, \quad \gamma_T \gg \gamma_M.$$

(iv) We assumed the following restrictions on the feedback gains v_x and v_p:

$$0 < \frac{\gamma_T}{\gamma_T + 4v_p} \ll 1,$$

$$0 < \frac{\omega_T - 2v_x}{\omega_T} \ll 1,$$

$$0 < \frac{\gamma_T g_{MT}^2 \omega_T^2}{\omega_M} \ll \chi^2.$$

The text below shows that all of these assumptions are experimentally accessible. Indeed, it can be verified that the system parameters given in Eqs. (29) and (30) satisfy all of these assumptions.

To show the validity of our strategy, let us show some numerical examples. The system parameters are chosen as [46]

$$L = 3.38 \times 10^{-11} \text{ H}, \quad C = 7.4 \times 10^{17} \text{ F},$$

$$I_c = 10 \ \mu\text{A}, \quad m = 10^{-16} \text{ kg}, \quad \eta = 0.6,$$

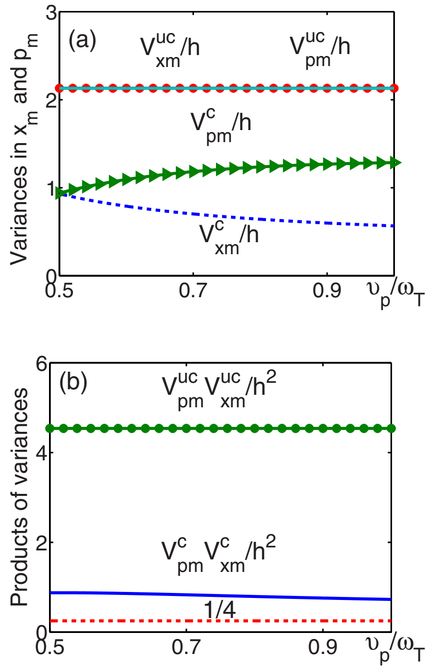

FIG. 3. (Color online) Squeezing the position fluctuations of the beam with the parameters given in Eqs. (29)–(31). (a) Variances of the position and momentum of the beam (in units of $\hbar$) versus the normalized control parameter $\tilde{\upsilon}_p = \upsilon_p/\omega_T$. Recall that υ_p is the linear feedback gain [see Eq. (19)]. The green line with triangles and the blue dashed line represent, respectively, the controlled variances of the position $V^c_{x_M}/\hbar$ and momentum $V^c_{p_M}/\hbar$ of the beam. The red line with asterisks and the blue solid line represent the uncontrolled variances $V^{uc}_{x_M}/\hbar$ and $V^{uc}_{p_M}/\hbar$ of the beam, which coincide because the beam without control is in a coherent thermal state with equal variances of position and momentum. (b) Products of the variances (in units of $\hbar^2$) versus the normalized control parameter $\tilde{\upsilon}_p = \upsilon_p/\omega_T$. The green line with asterisks and the blue solid line denote the uncontrolled trajectory $V^{uc}_{x_M}V^{uc}_{p_M}/\hbar^2$ and the controlled trajectory $V^c_{x_M}V^c_{p_M}/\hbar^2$, respectively. The red dashed line at 1/4 represents the Heisenberg uncertainty limit $\hbar^2/4$.

$$\omega_M/2\pi = 1 \text{ GHz}, \quad Bl = 1 \text{ T } \mu\text{m},$$

$$Q = 10^4, \quad T = 100 \text{ mK}, \quad \phi_e = 0, \quad \gamma_{S\varphi} = 0,$$

$$\gamma_{Sr}/2\pi = 100 \text{ MHz}, \quad \gamma_T/2\pi = 20 \text{ MHz},$$

$$g_{ST}/2\pi = 20 \text{ MHz}, \quad \omega_T/2\pi = 4.3 \text{ GHz}. \tag{29}$$

From the above parameters, it can be calculated that

$$\gamma_M/2\pi \approx 0.1 \text{ MHz}, \quad \omega_S/2\pi \approx 6.3 \text{ GHz},$$

$$g_{MS}/2\pi \approx 73 \text{ MHz}, \quad g_{MT}/2\pi \approx 4.9 \text{ MHz}. \tag{30}$$

In our numerical results, the stationary variances are calculated from the dynamic equation [Eq. (22)], and the feedback control parameters υ_x and υ_p are chosen to satisfy Eq. (26). In fact, in Fig. 3, we choose υ_x and υ_p such that

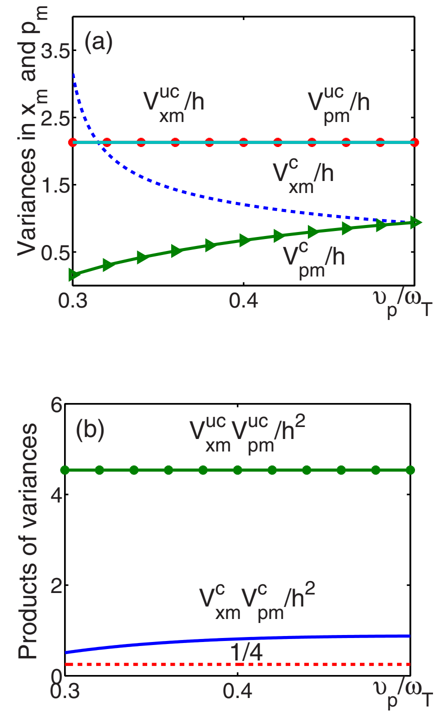

FIG. 4. (Color online) Squeezing the momentum fluctuations of the beam with the parameters given in Eqs. (29), (30), and (32). (a) Variances of the position and momentum of the beam (in units of $\hbar$) versus the normalized control parameter $\tilde{\upsilon}_p = \upsilon_p/\omega_T$. The green line with triangles and the blue dashed line represent, respectively, the controlled variances of the position $V^c_{x_M}/\hbar$ and momentum $V^c_{p_M}/\hbar$ of the beam. The red line with asterisks and the blue solid line represent the uncontrolled variances $V^{uc}_{x_M}/\hbar$ and $V^{uc}_{p_M}/\hbar$ of the beam, which coincide because the beam without control is in a coherent thermal state with equal variances of position and momentum. (b) Products of the variances (in units of $\hbar^2$) versus the normalized control parameter $\tilde{\upsilon}_p = \upsilon_p/\omega_T$. The green line with asterisks and the blue solid line denote the uncontrolled trajectory $V^{uc}_{x_M}V^{uc}_{p_M}/\hbar^2$ and the controlled trajectory $V^c_{x_M}V^c_{p_M}/\hbar^2$, respectively. The red dashed line at 1/4 represents the Heisenberg uncertainty limit $\hbar^2/4$.

$$\upsilon_x = 0.5\omega_T, \quad 0.5 \le \frac{\upsilon_p}{\omega_T} \le 1. \tag{31}$$

In this case, we have $\upsilon_p^2 \ge \upsilon_x^2$. Then, from Eqs. (27) and (28), it can be verified that $V^c_{x_M} \le V^c_{p_M}$, which coincides with the numerical results in Fig. 3(a) (the blue dashed line for $V^c_{x_M}/\hbar$ is below the green triangular line for $V^c_{p_M}/\hbar$). It means that the fluctuation of the position of the beam is squeezed. Meanwhile, the numerical results in Fig. 3(b) show that the variances $V^c_{x_M}$ and $V^c_{p_M}$ under control are much smaller than the variances $V^{uc}_{x_M}$ and $V^{uc}_{p_M}$ without control, which means that the designed feedback control reduces the variances of the position and momentum of the beam. The product of the variances under control $V^c_{x_M}V^c_{p_M}$ could even be reduced to be close to the Heisenberg uncertainty limit $\hbar^2/4$.

In Fig. 4, we choose υ_x and υ_p such that

$$\upsilon_x = 0.5\omega_T, \quad 0.3 \le \frac{\upsilon_p}{\omega_T} \le 0.5. \tag{32}$$

In this case, we can calculate from Eqs. (27) and (28) that $V^c_{x_M} \geq V^c_{p_M}$, which coincides with the numerical results in Fig. 4(a) (the green triangular line for $V^c_{p_M}/\hbar$ is below the blue dashed line for $V^c_{x_M}/\hbar$). It means that the fluctuations of the momentum of the beam are squeezed. More interestingly, the *numerical results* in Fig. 4(a) show that the variance of p_M is squeezed to be less than the standard quantum limit, i.e., $V^c_{p_M} < \hbar/2$. Numerical results in Fig. 4(b) show that the product $V^c_{x_M}V^c_{p_M}$ of the controlled variances is much smaller than the product $V^{uc}_{x_M}V^{uc}_{p_M}$ of the uncontrolled variances, which means that the variances of the position and momentum of the beam could be reduced under the designed feedback control. Indeed, as shown in Fig. 4(b), the product of the variances could be reduced to be close to the Heisenberg uncertainty limit $\hbar^2/4$.

B. Cooling

Further, let us investigate the cooling of the fluctuations of the nanomechanical beam. The cooling effect can be estimated by the average photon number of the nanomechanical beam,

$$\begin{aligned}\bar{n} &= E_{dW}(\langle b^\dagger b\rangle)\\ &= \frac{1}{2\hbar}(V_{x_M}+V_{p_M}) - \frac{1}{2} + \frac{1}{2\hbar}(V_{\langle x_M\rangle}+V_{\langle p_M\rangle}) + \frac{1}{2\hbar}(\bar{x}_M^2+\bar{p}_M^2),\end{aligned} \tag{33}$$

with

$$\bar{x}_M = E_{dW}(\langle x_M\rangle), \quad \bar{p}_M = E_{dW}(\langle p_M\rangle),$$

$$V_{\langle x_M\rangle} = E_{dW}(\langle x_M\rangle^2) - \bar{x}_M^2,$$

$$V_{\langle p_M\rangle} = E_{dW}(\langle p_M\rangle^2) - \bar{p}_M^2.$$

Here, E_{dW} means that the expectations and variances of $\langle x_M\rangle$ and $\langle p_M\rangle$ are about the Wiener noise dW.

From the system parameters given in Eqs. (29) and (30), it can be verified that the controlled stationary expectations $\bar{x}^c_M$, $\bar{p}^c_M$ and the classical fluctuations $V^c_{\langle x_M\rangle}$, $V^c_{\langle p_M\rangle}$ satisfy

$$\bar{x}^c_M = \bar{p}^c_M = 0, \quad V^c_{\langle x_M\rangle} \ll V^c_{x_M}, \quad V^c_{\langle p_M\rangle} \ll V^c_{p_M}.$$

Thus, from Eqs. (27) and (33), the controlled stationary average photon number can be estimated as

$$\bar{n}^c \approx \frac{1}{2\hbar}(V^c_{x_M}+V^c_{p_M}) - \frac{1}{2} \approx \frac{1}{4}\left(\sqrt{\frac{\xi}{\eta}} + \frac{1}{\sqrt{\xi\eta}}\right) - \frac{1}{2}, \tag{34}$$

which, under the parameters given in Eqs. (29)–(32), is smaller than the uncontrolled stationary average photon number,

$$\bar{n}^{uc} \approx \frac{1}{2\hbar}(V^{uc}_{x_M}+V^{uc}_{p_M}) - \frac{1}{2} \approx \bar{n}_M,$$

where $\bar{n}_M$ is given in Eq. (11).

Alternatively, we can use an effective temperature T_{eff} to quantify the cooling effect which is defined by

$$\bar{n} = \frac{1}{e^{\hbar\omega_M/k_B T_{\text{eff}}} - 1},$$

or, equivalently,

$$T_{\text{eff}} = \frac{\hbar\omega_M}{k_B \ln\left(\frac{\bar{n}+1}{\bar{n}}\right)}. \tag{35}$$

The controlled stationary effective temperature T^c_{eff} can be estimated as follows:

$$T^c_{\text{eff}} \approx \frac{\hbar\omega_M}{k_B \ln\left(\frac{\sqrt{\xi/\eta}+\sqrt{1/\xi\eta}+2}{\sqrt{\xi/\eta}+\sqrt{1/\xi\eta}-2}\right)}. \tag{36}$$

We now give some physical interpretations of our cooling strategy. There are two competing processes that determine the stationary effective temperature of the nanomechanical beam. The cooling process is provided by the leakage of the transmission line resonator, whose energy gap is larger than k_BT such that the thermal excitation from the environment could be negligible. Energy flows from the beam to the transmission line resonator via the coupling between them, and then it is dissipated via the leakage of the transmission line resonator. An opposing heating process is provided by the thermal excitation of the beam from the environment. Without applying quantum feedback control on the transmission line resonator, the cooling process of the beam is weak compared with the heating process, which leads to the failure of cooling. When we apply quantum feedback control and adjust the control parameters to be in the region given by Eq. (26), the decay of the beam caused by the leakage from the transmission line resonator is enhanced to overwhelm the heating process. Thus, the nanomechanical beam is effectively cooled.

To show the validity of our proposal, let us show some numerical examples. The system parameters are chosen as in Eqs. (29) and (30), and the feedback control parameters υ_x and υ_p are chosen such that

$$\upsilon_x = 0.5\omega_T, \quad 0.3 \leq \frac{\upsilon_p}{\omega_T} \leq 1. \tag{37}$$

The numerical results in Fig. 5 show that the average photon number and the effective temperature of the beam under control are reduced compared with the uncontrolled case. It means that our strategy can indeed effectively cool the motion of the beam. With the parameters given in Eqs. (29), (30), and (37), the minimum average photon number that can be reached is about 0.43, corresponding to an effective temperature $T^c_{\text{eff}} \approx 6.3$ mK. Further calculations show that the minimum average photon number that can be reached decreases when we increase the feedback gain υ_p. When the feedback gain υ_p is large enough such that $\upsilon_p \gg \upsilon_x$, the minimum average photon number can be estimated from Eqs. (26), (27), and (34) as

$$\bar{n}^c \approx \frac{1}{4\sqrt{\eta}}\left(\sqrt{\frac{\omega_M^-}{\omega_M^+}} + \sqrt{\frac{\omega_M^+}{\omega_M^-}}\right) - \frac{1}{2} \approx 0.25, \tag{38}$$

corresponding to an effective temperature $T^c_{\text{eff}} \approx 4.7$ mK, where $\omega_M^{\pm}$ are defined by

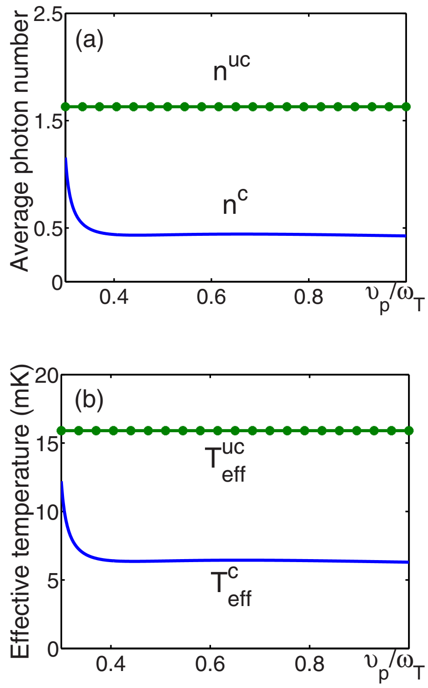

FIG. 5. (Color online) Cooling the nanomechanical beam for (a) the average photon number $\bar{n}$, and (b) the effective temperature T_{eff} versus the normalized control parameter $\tilde{\upsilon}_p = \upsilon_p/\omega_T$. The blue solid lines representing the average photon number n^c and effective temperatures T_{eff}^c under control are below the green lines with asterisks representing the corresponding average photon number n^{uc} and effective temperature T_{eff}^{uc} without control, which means that the designed feedback control could effectively cool the fluctuations of the beam induced by thermal noises.

$$\omega_M^{\pm} = \omega_M \pm \frac{2\omega_T g_{MT}^2}{\gamma_T^2}. \tag{39}$$

Note that the cooling limit of our proposal is still an open question. The main difficulty comes from the fact that the parameter region given in Eq. (26) is too restricted. If the feedback gains υ_x and υ_p do not lie in this region, we cannot obtain an analytic expression like Eq. (27), and thus it is hard to obtain the achievable cooling limit in this case. However, at least, the achievable cooling limit of our proposal is restricted by the Heisenberg uncertainty limit under imperfect quantum weak measurements (see, e.g., Ref. [64]), which can be written as

$$\bar{n}^c = \frac{1}{2}\left(\frac{1}{\sqrt{\eta}} - 1\right), \tag{40}$$

corresponding to the minimum uncertainty state under imperfect quantum weak measurements with

$$V_{x_M}^c = V_{p_M}^c = \frac{1}{2\sqrt{\eta}}. \tag{41}$$

VI. CONCLUSIONS

In summary, we have investigated the possibility of using quantum feedback control to squeeze and cool down the fluctuations of a nanomechanical beam embedded in a coupled transmission line resonator-SQUID-mechanical beam quantum circuit. The leakage of the electromagnetic field from the transmission line resonator is detected using homodyne measurement, and the measurement output is then used to design a quantum feedback control signal to drive the electromagnetic field in the transmission line resonator. The designed quantum feedback control protocol indirectly affects the motion of the beam by the inductive coupling between the transmission line resonator and the beam via the rf SQUID. After adiabatically eliminating the degrees of freedom of the rf SQUID and the transmission line resonator, the quantum feedback control results in a two-photon term in the effective Hamiltonian and additional damping terms for the beam, which lead to squeezing and cooling for the beam. By varying the feedback control parameters, the variance of either the position or momentum of the beam could be squeezed, and the variance of the momentum of the beam could even be squeezed to be less than the standard quantum limit $\hbar/2$. Meanwhile, the average photon number (or, equivalently, the effective temperature) of the beam could be reduced effectively by applying control, compared with the uncontrolled case.

Although the thermal motion of the beam could be effectively suppressed by the proposed quantum feedback control protocol, our calculations show that the beam has not achieved the ground state. Further work will focus on extending our results to explore ways to further lower the achievable effective temperature or even attain the ground state of the beam. Another possible direction is to consider nonlinear effects [65] of the nanomechanical oscillator, which may affect the achievable cooling temperature and the squeezing effects induced by the quantum feedback control.

ACKNOWLEDGMENTS

We thank Dr. S. Ashhab for his great help on this work. J.Z would like to thank Dr. N. Yamamoto for helpful discussions. F.N. acknowledges partial support from the National Security Agency (NSA), Laboratory Physical Science (LPS), (U.S.) Army Research Office (ARO), National Science Foundation (NSF) under Grant No. EIA-0130383, and JSPS-RFBR under Grant No. 06-02-91200. J.Z. was supported by the National Natural Science Foundation of China under Grant Nos. 60704017, 60635040, and 60674039 and the China Postdoctoral Science Foundation.

APPENDIX A: DERIVATION OF THE QUANTUM STOCHASTIC DIFFERENTIAL EQUATION [EQ. (10)]

Let X be an operator of the coupled beam-SQUID-resonator system, then the Heisenberg equation for X can be written as

$$\begin{aligned} dX &= -\frac{i}{\hbar}[X, H_{\text{tot}}dt] - \frac{1}{2\hbar^2}[[X, H_{\text{tot}}dt], H_{\text{tot}}dt] \\ &= -\frac{i}{\hbar}[X, H_{\text{eff}}]dt + dL_{pT}(X) + dL_{eT}(X) \\ &\quad + dL_{eM}(X) + dL_{eS,\varphi}(X) + dL_{eS,r}(X), \end{aligned} \tag{A1}$$

where

$$dL_{\alpha}(X) = -\frac{i}{\hbar}[X,H_{\alpha}dt] - \frac{1}{2\hbar^2}[[X,H_{\alpha}dt],H_{\alpha}dt],$$

and

$$H_{pT} = \hbar\int d\omega[g_{pT}^{*}(\omega)c_{pT}^{\dagger}a + g_{pT}(\omega)a^{\dagger}c_{pT}],$$

$$H_{eT} = \hbar\int d\omega[g_{eT}^{*}(\omega)c_{eT}^{\dagger}a + g_{eT}(\omega)a^{\dagger}c_{eT}],$$

$$H_{eM} = \hbar\int d\omega[g_{eM}^{*}(\omega)c_{eM}^{\dagger}b + g_{eM}(\omega)b^{\dagger}c_{eM}],$$

$$H_{eS,\varphi} = \hbar\int d\omega[g_{eS,\varphi}^{*}(\omega)c_{eS}^{\dagger}\sigma_z + g_{eS,\varphi}(\omega)\sigma_z c_{eS}],$$

$$H_{eS,r} = \hbar\int d\omega[g_{eS,r}^{*}(\omega)c_{eS}^{\dagger}\sigma_- + g_{eS,r}(\omega)\sigma_+ c_{eS}].$$

Here, we expand dX to second-order differential terms because we may meet quantum Wiener increments and the second-order terms cannot be omitted.

In order to eliminate the environmental degrees of freedom corresponding to $c_{pT}(\omega)$, we first solve the equation for $c_{pT}(\omega)$,

$$\dot{c}_{pT}(\omega) = -\frac{i}{\hbar}[c_{pT}(\omega),H_{\text{tot}}] = -i\omega c_{pT}(\omega) - ig_{pT}^{*}(\omega)a,$$

to obtain

$$c_{pT}(\omega,t) = \int_{t_0}^{t} dt' e^{-i\omega(t-t')}(-ig_{pT}^{*}(\omega))a(t') + e^{-i\omega(t-t_0)}c_{pT}(\omega,t_0). \tag{A2}$$

Further, let us introduce the so-called first Markovian approximation to omit the frequency dependence of the coupling strength [45],

$$g_{pT}(\omega) = \sqrt{\frac{\gamma_{pT}}{2\pi}}e^{i\phi_{pT}}, \tag{A3}$$

where γ_{pT} and ϕ_{pT} are independent of ω.

By substituting Eqs. (A2) and (A3) into $dL_{pT}(X)$, we have

$$\begin{aligned}-\frac{i}{\hbar}[X,H_{pT}dt] &= \left\{\int d\omega|g_{pT}(\omega)|^2\int_{t_0}^{t} dt' e^{-i\omega(t-t')}(a^{\dagger}(t')[X,a] + a(t')[a^{\dagger},X])\right\}dt \\ &\quad - ig_{pT}^{*}\int d\omega e^{i\omega(t-t_0)}c_{pT}^{\dagger}(\omega,t_0)[X,a]dt + ig_{pT}[a^{\dagger},X]\int d\omega e^{-i\omega(t-t_0)}c_{pT}(\omega,t_0)dt \\ &= \frac{\gamma_{pT}}{2}(a^{\dagger}[X,a] - a[X,a^{\dagger}])dt + (-i\sqrt{\gamma_{pT}}e^{-i\phi_{pT}}d\tilde{A}_{\text{in}}^{\dagger})[X,a] + [a^{\dagger},X](i\sqrt{\gamma_{pT}}e^{i\phi_{pT}}d\tilde{A}_{\text{in}}),\end{aligned}$$

where

$$d\tilde{A}_{\text{in}} = \left(\frac{1}{\sqrt{2\pi}}\int d\omega e^{-i\omega(t-t_0)}c_{pT}(\omega,t_0)\right)dt$$

is the input quantum noise such that

$$d\tilde{A}_{\text{in}}d\tilde{A}_{\text{in}}^{\dagger} = (\bar{n}(\omega_T)+1)dt,$$

$$d\tilde{A}_{\text{in}}^{\dagger}d\tilde{A}_{\text{in}} = \bar{n}(\omega_T)dt,$$

$$d\tilde{A}_{\text{in}}d\tilde{A}_{\text{in}} = d\tilde{A}_{\text{in}}^{\dagger}d\tilde{A}_{\text{in}}^{\dagger} = 0,$$

and

$$\bar{n}(\omega) = \frac{1}{e^{\hbar\omega/k_B T}-1}.$$

Further, we have

$$\begin{aligned}-\frac{1}{2\hbar^2}[[X,H_{pT}dt],H_{pT}dt] &= -\frac{\gamma_{pT}}{2}\bar{n}(\omega_T)[[X,a],a^{\dagger}]dt \\ &\quad - \frac{\gamma_{pT}}{2}(\bar{n}(\omega_T)+1)[[X,a^{\dagger}],a]dt.\end{aligned}$$

From the above analysis, it can be calculated that

$$\begin{aligned}dL_{pT}(X) &= -\frac{i}{\hbar}[X,H_{pT}dt] - \frac{1}{2\hbar^2}[[X,H_{pT}],H_{pT}dt] \\ &= \frac{\gamma_{pT}}{2}(\bar{n}(\omega_T)+1)(a^{\dagger}[X,a] + [a^{\dagger},X]a) \\ &\quad + \frac{\gamma_{pT}}{2}\bar{n}(\omega_T)(a[X,a^{\dagger}] + [a,X]a^{\dagger}) \\ &\quad + \sqrt{\gamma_{pT}}dA_{\text{in}}^{\dagger}[X,a] + \sqrt{\gamma_{pT}}[a^{\dagger},X]dA_{\text{in}},\end{aligned}$$

where $dA_{\text{in}} = ie^{i\phi_{pT}}d\tilde{A}_{\text{in}}$.

With the same analysis, we can calculate $dL_{eT}(X)$, $dL_{eM}(X)$, $dL_{eS,\varphi}(X)$, and $dL_{eS,r}(X)$. Furthermore, under the condition that $\hbar\omega_S$, $\hbar\omega_T \gg k_B T$, we have $\bar{n}(\omega_S)$, $\bar{n}(\omega_T)\approx 0$. Thus, by substituting the above results into Eq. (A1), averaging over the fluctuations caused by the thermal noises, and assuming that

$$\gamma_T = \gamma_{pT} + \gamma_{eT}, \quad \eta = \frac{\gamma_{pT}}{\gamma_{pT}+\gamma_{eT}},$$

we can obtain the quantum stochastic differential equation [Eq. (10)].

In order to calculate the measurement output of the homodyne detection, let us recall that the input and output detection noises should be

$$d\tilde{A}_{\rm in} = \left(\frac{1}{\sqrt{2\pi}}\int d\omega e^{-i\omega(t-t_0)} c_{pT}(\omega,t_0)\right)dt,$$

$$d\tilde{A}_{\rm out} = \left(\frac{1}{\sqrt{2\pi}}\int d\omega e^{-i\omega(t-t_0)} c_{pT}(\omega,t_1)\right)dt,$$

where the time t_0 is an instant before the measurement commences and the time t_1 is another instant after the measurement has finished. The measurement output is related to $d\tilde{A}_{\rm out}$ by

$$dY_t = e^{-i\phi_{LO}} d\tilde{A}^\dagger_{\rm out} + e^{i\phi_{LO}} d\tilde{A}_{\rm out},$$

where ϕ_{LO} is an adjustable phase introduced by the local oscillator of the homodyne detection. From Eq. (A2), we have

$$\begin{aligned} c_{pT}(\omega,t) &= -i\sqrt{\gamma_{pT}} e^{-i\phi_{pT}} \frac{1}{\sqrt{2\pi}}\int_{t_0}^{t} dt' e^{-i\omega(t-t')} a(t') \\ &\quad + e^{-i\omega(t-t_0)} c_{pT}(\omega,t_0) \\ &= -i\sqrt{\gamma_{pT}} e^{-i\phi_{pT}} \frac{1}{\sqrt{2\pi}}\int_{t_1}^{t} dt' e^{-i\omega(t-t')} a(t') \\ &\quad + e^{-i\omega(t-t_1)} c_{pT}(\omega,t_1). \end{aligned}$$

Thus, it can be calculated that

$$d\tilde{A}_{\rm out} - d\tilde{A}_{\rm in} = -i\sqrt{\gamma_{pT}} e^{-i\phi_{pT}} a(t)dt,$$

from which it can be shown that

$$\begin{aligned} dY_t &= i\sqrt{\gamma_{pT}} a^\dagger e^{i(\phi_{pT}-\phi_{LO})} - i\sqrt{\gamma_{pT}} a e^{-i(\phi_{pT}-\phi_{LO})} \\ &\quad + e^{-i\phi_{LO}} d\tilde{A}^\dagger_{\rm in} + e^{i\phi_{LO}} d\tilde{A}_{\rm in}. \end{aligned}$$

By setting $\phi_{LO}=\phi_{pT}+\pi/2$, we have

$$\begin{aligned} dY_t &= \sqrt{\gamma_{pT}}(a^\dagger + a) + (ie^{i\phi_{pT}} d\tilde{A}_{\rm in} - ie^{-i\phi_{pT}} d\tilde{A}^\dagger_{\rm in}) \\ &= \sqrt{\eta\gamma_T}(a^\dagger + a) + (dA_{\rm in} + dA^\dagger_{\rm in}). \end{aligned}$$

APPENDIX B: DERIVATION OF THE REDUCED STOCHASTIC MASTER EQUATION [EQ. (22)]

Under the semiclassical approximation, we can obtain Maxwell-Bloch-type equations from the stochastic master equation [Eq. (16)] for the coupled beam-SQUID-resonator system (see, e.g., Ref. [66]). Further, in the large-detuning regime [see Eq. (9)], we have

$$\frac{g_{MS}^2}{\Delta_{MS}}, \ \frac{g_{ST}^2}{\Delta_{ST}}, \ g_{MT} \ll \omega_M, \ \omega_T, \ \omega_S, \tag{B1}$$

where

$$g_{MT} = g_{MS} g_{ST}\left(\frac{1}{\Delta_{MS}} + \frac{1}{\Delta_{ST}}\right). \tag{B2}$$

Then, we can omit the frequency shifts of the beam, the rf SQUID, and the transmission line resonator induced by the coupling between them. Under this condition, the Maxwell-Bloch-type equations for the coupled system obtained from the stochastic master equation [Eq. (16)] can be expressed as

$$\begin{aligned} \langle\dot{\sigma}_x\rangle &= -\omega_S\langle\sigma_y\rangle - \left(\frac{\gamma_{Sr}}{2} + 2\gamma_{S\varphi}\right)\langle\sigma_x\rangle, \\ \langle\dot{\sigma}_y\rangle &= \omega_S\langle\sigma_x\rangle - \left(\frac{\gamma_{Sr}}{2} + 2\gamma_{S\varphi}\right)\langle\sigma_y\rangle, \\ \langle\dot{\sigma}_z\rangle &= -\gamma_{Sr}\langle\sigma_z\rangle - \gamma_{Sr}, \\ \langle\dot{b}\rangle &= -i\omega_M\langle b\rangle + g_{MT}\langle\sigma_z\rangle\langle a\rangle - \frac{\gamma_M}{2}\langle b\rangle, \\ d\langle a\rangle &= -i\omega_T\langle a\rangle dt - g_{MT}\langle\sigma_z\rangle\langle b\rangle dt - \frac{\gamma_T}{2}\langle a\rangle dt - iu(t)dt \\ &\quad + \sqrt{\frac{\eta\gamma_T}{\hbar}}\left(V_{x_T} + iC_{x_T p_T} - \frac{\hbar}{2}\right)dW, \end{aligned} \tag{B3}$$

where dW has been given in Eq. (17),

$$V_{x_T} = \langle x_T^2\rangle - \langle x_T\rangle^2, \quad V_{p_T} = \langle p_T^2\rangle - \langle p_T\rangle^2$$

are the variances of the normalized position and momentum operators of the transmission line resonator given by Eq. (20), and

$$C_{x_T p_T} = \left\langle \frac{x_T p_T + p_T x_T}{2}\right\rangle - \langle x_T\rangle\langle p_T\rangle$$

is the corresponding symmetric covariance. Under the semiclassical approximation and condition (B1), V_{x_T}, V_{p_T}, and $C_{x_T p_T}$ can be given by the following equations:

$$\begin{aligned} \dot{V}_{x_T} &= -\gamma_T V_{x_T} + 2\omega_T C_{x_T p_T} + \hbar\gamma_T/2 - 2\eta\gamma_T(V_{x_T} - \hbar/2)^2, \\ \dot{V}_{p_T} &= -\gamma_T V_{p_T} - 2\omega_T C_{x_T p_T} + \hbar\gamma_T/2 - 2\eta\gamma_T C_{x_T p_T}^2, \\ \dot{C}_{x_T p_T} &= -\gamma_T C_{x_T p_T} + \omega_T V_{p_T} - \omega_T V_{x_T} - 2\eta\gamma_T(V_{x_T} - \hbar/2)C_{x_T p_T}. \end{aligned} \tag{B4}$$

By substituting feedback control (19) into Eq. (B3), we can replace the last equation in Eq. (B3) by the following equation:

$$d\langle a\rangle = -i\omega_T\langle a\rangle dt - g_{MT}\langle\sigma_z\rangle\langle b\rangle dt - \frac{\gamma_T}{2}\langle a\rangle dt + i\upsilon_x\langle a + a^\dagger\rangle dt - i\upsilon_p\langle -ia + ia^\dagger\rangle dt + \sqrt{\frac{\eta\gamma_T}{\hbar}}\left(V_{x_T} + iC_{x_Tp_T} - \frac{\hbar}{2}\right)dW. \tag{B5}$$

If the damping rates of the rf SQUID and the transmission line resonator are large enough such that

$$\frac{\gamma_{Sr}}{2} + 2\gamma_{S\varphi}, \quad \gamma_T \gg \gamma_M\bar{n}_M, \tag{B6}$$

we can adiabatically eliminate [59,60] the degrees of freedom of the rf SQUID and the transmission line resonator to obtain the reduced equation of the beam. In fact, in this case, we can obtain the following stationary variances from Eq. (B4):

$$V_{x_T} = V_{p_T} = \frac{\hbar}{2}, \quad C_{x_Tp_T} = 0,$$

from which it can be verified that the fluctuation in Eq. (B5) will tend to zero. Then, in the Heisenberg picture, one finds from the stationary solution of Eqs. (B3) and (B5) that

$$\sigma_z \sim -1, \quad a \sim C_1 b + C_2 b^\dagger, \tag{B7}$$

where C_1 are C_2 are given by Eq. (24). Substituting Eq. (B7) into Eq. (16), we can obtain the reduced stochastic master equation [Eq. (22)] for the nanomechanical beam.

[1] K. C. Schwab and M. L. Roukes, Phys. Today **58**(7), 36 (2005).
[2] M. Blencowe, Phys. Rep. **395**, 159 (2004).
[3] K. L. Ekinci and M. L. Roukes, Rev. Sci. Instrum. **76**, 061101 (2005).
[4] A. N. Cleland, *Foundations of Nanomechanics: From Solid-State Theory to Device Applications* (Springer-Verlag, Berlin, 2002).
[5] E. Buks and B. Yurke, Phys. Rev. E **74**, 046619 (2006).
[6] S. Savel'ev, X. Hu, and F. Nori, New J. Phys. **8**, 105 (2006); S. Savel'ev, A. L. Rakhmanov, X. Hu, A. Kasumov, and F. Nori, Phys. Rev. B **75**, 165417 (2007); S. Savel'ev and F. Nori, *ibid.* **70**, 214415 (2004).
[7] S. Mancini, D. Vitali, and P. Tombesi, Phys. Rev. Lett. **90**, 137901 (2003); D. Vitali, S. Gigan, A. Ferreira, H. R. Böhm, P. Tombesi, A. Guerreiro, V. Vedral, A. Zeilinger, and M. Aspelmeyer, *ibid.* **98**, 030405 (2007).
[8] I. Mahboob and H. Yamaguchi, Nat. Nanotechnol. **3**, 275 (2008).
[9] L. F. Wei, Y. X. Liu, C. P. Sun, and F. Nori, Phys. Rev. Lett. **97**, 237201 (2006).
[10] W. Marshall, C. Simon, R. Penrose, and D. Bouwmeester, Phys. Rev. Lett. **91**, 130401 (2003).
[11] X. M. H. Huang, C. A. Zorman, M. Mehregany, and M. L. Roukes, Nature (London) **421**, 496 (2003).
[12] A. Gaidarzhy, G. Zolfagharkhani, R. L. Badzey, and P. Mohanty, Phys. Rev. Lett. **94**, 030402 (2005); **95**, 248902 (2005); K. C. Schwab, M. P. Blencowe, M. L. Roukes, A. N. Cleland, S. M. Girvin, G. J. Milburn, and K. L. Ekinci, *ibid.* **95**, 248901 (2005).
[13] C. H. Metzger and K. Karrai, Nature (London) **432**, 1002 (2004).
[14] A. Naik, O. Buu, M. D. LaHaye, A. D. Armour, A. A. Clerk, M. P. Blencowe, and K. C. Schwab, Nature (London) **443**, 193 (2006).
[15] S. Gigan, H. R. Böhm, M. Paternostro, F. Blaser, G. Langer, J. B. Hertzberg, K. C. Schwab, D. Bäuerle, M. Aspelmeyer, and A. Zeilinger, Nature (London) **444**, 67 (2006).
[16] O. Arcizet, P.-F. Cohadon, T. Briant, M. Pinard, and A. Heidmann, Nature (London) **444**, 71 (2006).
[17] A. Schliesser, P. Del'Haye, N. Nooshi, K. J. Vahala, and T. J. Kippenberg, Phys. Rev. Lett. **97**, 243905 (2006).
[18] T. J. Kippenberg, H. Rokhsari, T. Carmon, A. Scherer, and K. J. Vahala, Phys. Rev. Lett. **95**, 033901 (2005).
[19] T. Corbitt, C. Wipf, T. Bodiya, D. Ottaway, D. Sigg, N. Smith, S. Whitcomb, and N. Mavalvala, Phys. Rev. Lett. **99**, 160801 (2007).
[20] M. Bhattacharya and P. Meystre, Phys. Rev. Lett. **99**, 073601 (2007).
[21] D. Kleckner and D. Bouwmeester, Nature (London) **444**, 75 (2006).
[22] P. F. Cohadon, A. Heidmann, and M. Pinard, Phys. Rev. Lett. **83**, 3174 (1999).
[23] M. Poggio, C. L. Degen, H. J. Mamin, and D. Rugar, Phys. Rev. Lett. **99**, 017201 (2007).
[24] A. Schliesser, R. Rivière, G. Anetsberger, O. Arcizet, and T. J. Kippenberg, Nat. Phys. **4**, 415 (2008).
[25] I. Wilson-Rae, N. Nooshi, W. Zwerger, and T. J. Kippenberg, Phys. Rev. Lett. **99**, 093901 (2007).
[26] F. Marquardt, J. P. Chen, A. A. Clerk, and S. M. Girvin, Phys. Rev. Lett. **99**, 093902 (2007).
[27] C. Genes, D. Vitali, P. Tombesi, S. Gigan, and M. Aspelmeyer, Phys. Rev. A **77**, 033804 (2008).
[28] Y. D. Wang, K. Semba, and H. Yamaguchi, New J. Phys. **10**, 043015 (2008); Y. D. Wang, Y. Li, F. Xue, C. Bruder, and K. Semba, e-print arXiv:0812.0261; Y. Li, Y. D. Wang, F. Xue, and C. Bruder, Phys. Rev. B **78**, 134301 (2008).
[29] M. Grajcar, S. Ashhab, J. R. Johansson, and F. Nori, Phys. Rev. B **78**, 035406 (2008).
[30] L. Tian, e-print arXiv:0809.4459; K. Jaehne, K. Hammerer, and M. Wallquist, New J. Phys. **10**, 095019 (2008).
[31] A. Naik, O. Buu, M. D. LaHaye, A. D. Armour, A. A. Clerk, M. P. Blencowe, and K. C. Schwab, Nature (London) **443**, 193 (2006).
[32] A. Hopkins, K. Jacobs, S. Habib, and K. C. Schwab, Phys. Rev. B **68**, 235328 (2003).
[33] I. Wilson-Rae, P. Zoller, and A. Imamoglu, Phys. Rev. Lett. **92**, 075507 (2004).
[34] N. Lambert and F. Nori, Phys. Rev. B **78**, 214302 (2008); S. H. Ouyang, J. Q. You, and F. Nori, *ibid.* **79**, 075304 (2009).

[35] I. Martin, A. Shnirman, L. Tian, and P. Zoller, Phys. Rev. B **69**, 125339 (2004).
[36] P. Zhang, Y. D. Wang, and C. P. Sun, Phys. Rev. Lett. **95**, 097204 (2005).
[37] J. Q. You, Y. X. Liu, and F. Nori, Phys. Rev. Lett. **100**, 047001 (2008).
[38] J. Q. You, Y. X. Liu, C. P. Sun, and F. Nori, Phys. Rev. B **75**, 104516 (2007); J. Hauss, A. Fedorov, C. Hutter, A. Shnirman, and G. Schön, Phys. Rev. Lett. **100**, 037003 (2008).
[39] A. Vinante, M. Bignotto, M. Bonaldi, M. Cerdonio, L. Conti, P. Falferi, N. Liguori, S. Longo, R. Mezzena, A. Ortolan, G. A. Prodi, F. Salemi, L. Taffarello, G. Vedovato, S. Vitale, and J.-P. Zendri, Phys. Rev. Lett. **101**, 033601 (2008).
[40] F. Xue, Y. D. Wang, Y. X. Liu, and F. Nori, Phys. Rev. B **76**, 205302 (2007).
[41] J. D. Teufel, J. W. Harlow, C. A. Regal, and K. W. Lehnert, Phys. Rev. Lett. **101**, 197203 (2008).
[42] S. Etaki, M. Poot, I. Mahboob, K. Onomitsu, H. Yamaguchi, and H. S. J. van der Zant, Nat. Phys. **4**, 785 (2008).
[43] J. Q. You and F. Nori, Phys. Rev. B **68**, 064509 (2003); J. Q. You, J. S. Tsai, and F. Nori, *ibid.* **68**, 024510 (2003).
[44] A. Blais, R. S. Huang, A. Wallraff, S. M. Girvin, and R. J. Schoelkopf, Phys. Rev. A **69**, 062320 (2004); J. Gambetta, A. Blais, M. Boissonneault, A. A. Houck, D. I. Schuster, and S. M. Girvin, *ibid.* **77**, 012112 (2008).
[45] M. P. Blencowe and E. Buks, Phys. Rev. B **76**, 014511 (2007).
[46] E. Buks and M. P. Blencowe, Phys. Rev. B **74**, 174504 (2006).
[47] E. Buks, S. Zaitsev, E. Segev, B. Abdo, and M. P. Blencowe, Phys. Rev. E **76**, 026217 (2007).
[48] R. Ruskov, K. Schwab, and A. N. Korotkov, Phys. Rev. B **71**, 235407 (2005).
[49] R. Migliore and A. Messina, Phys. Rev. B **72**, 214508 (2005).
[50] C. P. Sun, L. F. Wei, Y. X. Liu, and F. Nori, Phys. Rev. A **73**, 022318 (2006); M. Mariantoni, F. Deppe, A. Marx, R. Gross, F. K. Wilhelm, and E. Solano, Phys. Rev. B **78**, 104508 (2008).
[51] C. W. Gardiner and P. Zoller, *Quantum Noise*, 3rd ed. (Springer-Verlag, Berlin, 2004).
[52] J. M. Geremia, J. K. Stockton, and H. Mabuchi, Science **304**, 270 (2004); R. van Handel, J. K. Stockton, and H. Mabuchi, IEEE Trans. Autom. Control **50**, 768 (2005); J. M. Geremia, J. K. Stockton, A. C. Doherty, and H. Mabuchi, Phys. Rev. Lett. **91**, 250801 (2003).
[53] K. Jacobs and A. P. Lund, Phys. Rev. Lett. **99**, 020501 (2007); J. Combes and K. Jacobs, *ibid.* **96**, 010504 (2006); D. A. Steck, K. Jacobs, H. Mabuchi, T. Bhattacharya, and S. Habib, *ibid.* **92**, 223004 (2004).
[54] H. M. Wiseman and G. J. Milburn, Phys. Rev. Lett. **70**, 548 (1993); Phys. Rev. A **47**, 1652 (1993); **49**, 1350 (1994).
[55] A. C. Doherty and K. Jacobs, Phys. Rev. A **60**, 2700 (1999); A. C. Doherty, S. Habib, K. Jacobs, H. Mabuchi, and S. M. Tan, *ibid.* **62**, 012105 (2000).
[56] V. P. Belavkin, J. Multivariate Anal. **42**, 171 (1992); V. P. Belavkin, Commun. Math. Phys. **146**, 611 (1992); V. P. Belavkin, Theor. Probab. Appl. **38**, 573 (1993).
[57] L. Bouten, R. van Handel, and M. R. James, SIAM J. Control Optim. **46**, 2199 (2007); L. Bouten, M. Guta, and H. Maassen, J. Phys. A **37**, 3189 (2004); L. Bouten and R. van Handel, e-print arXiv:math-ph/0511021; *Quantum Stochastics and Information: Statistics, Filtering and Control*, edited by V. P. Belavkin and M. I. Guta (World Scientific, Singapore, 2008).
[58] N. Yamamoto, Phys. Rev. A **74**, 032107 (2006).
[59] D. F. Walls and G. J. Milburn, *Quantum Optics* (Springer-Verlag, Berlin, 1994).
[60] D. A. Steck, K. Jacobs, H. Mabuchi, S. Habib, and T. Bhattacharya, Phys. Rev. A **74**, 012322 (2006).
[61] X. Hu and F. Nori, Phys. Rev. Lett. **76**, 2294 (1996); **79**, 4605 (1997); Phys. Rev. B **53**, 2419 (1996); Physica B **263-264**, 16 (1999).
[62] X. Hu and F. Nori, *Squeezed Quantum States in Josephson Junctions* (University of Michigan, Ann Arbor, MI, 1996); X. Hu, Ph.D. Thesis, University of Michigan, 1996; see also http://www-personal.umich.edu/~nori/squeezed.html
[63] A. M. Zagoskin, E. Il'ichev, M. W. McCutcheon, J. F. Young, and F. Nori, Phys. Rev. Lett. **101**, 253602 (2008).
[64] N. Yamamoto and S. Hara, Phys. Rev. A **76**, 034102 (2007).
[65] K. Jacobs, Phys. Rev. Lett. **99**, 117203 (2007).
[66] H. Mabuchi, Phys. Rev. A **78**, 015801 (2008).